Hyperfine Interaction Induced *K*-type Doubling in the mmw Spectrum of $HS^{33}SH$

Axel H. Saleck and Gisbert Winnewisser
I. Physikalisches Institut, Universität zu Köln, Zülpicher Str. 77, D-50937 Köln

Z. Naturforsch. **50 a,** 1191–1198 (1995); received November 14, 1995

The rotational spectrum of the disulfane isotopomer $HS^{33}SH$ has been recorded and assigned between 70 and 300 GHz. In the analysis, rotational constants and ^{33}S hyperfine parameters are derived, the latter accounting for nuclear electric quadrupole as well as nuclear spin - rotation hyperfine interactions. The quadrupole constants are in qualitative agreement with a published ab-initio calculation. The electric field gradient principal axes are considerably rotated against the principal inertial axes, giving rise to off-diagonal elements in the electric field gradient tensor. In combination with the very small inertial asymmetry of the molecule, this causes the K-doubling in the lowest rotational levels to be dominated by the hyperfine structure rather than the inertial asymmetry contributions. By diagonalization of the quadrupole tensor, an estimate for the dihedral angle ($\eta \approx 94°$) can be obtained, in good agreement with a previous value.

1. Introduction

Disulfane, H_2S_2, is unique among asymmetric top molecules in that it is very close to an almost perfectly accidental prolate symmetric top as judged by the principal moments of inertia. Nevertheless, the skew chain geometry of the molecule gives rise to a perpendicular spectrum which a real prolate top cannot exhibit. H_2S_2 thus displays a rotational and rotation-vibration spectrum of a near symmetric top, but with asymmetric rotor selection rules. Previous experimental work was concerned with the rotational and vibrational spectra of different isotopomers, including D and ^{34}S substituted species (cf. [1] - [11]). These studies revealed a plethora of effects and provided the determination of a partial equilibrium structure [10, 11]. Ab initio calculations on the structure have been published by several authors ([12] - [17]). Among them, Palmer [17] has not only calculated ab-initio structures using a triple zeta valence + polarization (TZVP) basis of gaussian type orbitals, but also first theoretical values of the nuclear quadrupole coupling constants. From experiment, however, no data on ^{33}S containing disulfane isotopomers have been reported so far.

After the recent reinvestigation of the ^{33}S hyperfine structure (hfs) in $H_2{}^{33}S$ [18], we report in this paper the measurement and identification of the $HS^{33}SH$ rotational spectrum between 70 and 300 GHz. In the present analysis, rotational constants and ^{33}S hyperfine parameters are determined, the latter accounting for nuclear electric quadrupole as well as nuclear spin - rotation hyperfine interactions. In the discussion section, the relation between the hfs parameters and the molecular geometry will be presented.

2. Hamiltonian

The Hamiltonian used to describe the present rotational spectrum contains three terms as follows:

$$H = H_{\mathrm{Rot}} + H_{\mathrm{Q}} + H_{\mathrm{NSR}}, \qquad (1)$$

where the H_{Rot} denotes the rotational part of the Hamiltonian, H_{Q} the contribution due to nuclear quadrupole hyperfine interaction, and H_{NSR} the nuclear spin - rotation term.

The rotational part was already described in [9] where it has been employed for the analysis of the HSSH and $HS^{34}SH$ spectra. We use the same matrix elements of the prolate S-reduction here.

The $HS^{33}SH$ ground state rotational constants A_0, B_0, C_0 were estimated on the basis of equilibrium rotational constants A_e, B_e, C_e (obtained from

---

Reprint requests to Prof. Dr. G. Winnewisser.
Fax: 0221 / 470-5162.

0932-0784 / 95 / 1200-1191 $ 06.00 © – Verlag der Zeitschrift für Naturforschung, D-72072 Tübingen

the partial equilibrium structure [11] where the torsional contribution has been accounted for) by

$$X_0(S_{33}) = \frac{X_0^{\text{exp}}(S_{32})}{X_e(S_{32})} X_e(S_{33}) + \frac{1}{2}\left[X_0^{\text{exp}}(S_{34}) - \frac{X_0^{\text{exp}}(S_{32})}{X_e(S_{32})} X_e(S_{34})\right], \quad (2)$$

where $X = A, B, C, S_\alpha = HS^\alpha SH$, ${}^{\text{exp}}$ = determined from experiment. The centrifugal distortion constants have been predicted by averaging the corresponding HSSH and $HS^{34}SH$ values.

The hyperfine structure in a disulfane isotopomer is considered in this work for the first time. The matrix elements for the nuclear quadrupole hfs of an asymmetric top have been given in tensor notation by Bowater et al. [19]. In a prolate basis, we have

$$\begin{aligned}\langle J'K'IF|H_Q|JKIF\rangle &= \frac{1}{2}(-1)^{I+J'+F}\begin{Bmatrix} F & J' & I \\ 2 & I & J \end{Bmatrix} \\ &\times \sqrt{\frac{(I+1)(2I+1)(2I+3)}{I(2I-1)}} \sum_{q=-2}^{2} (-1)^{J'-K'} \quad (3) \\ &\times \sqrt{(2J+1)(2J'+1)} \begin{Bmatrix} J' & 2 & J \\ -K' & q & K \end{Bmatrix} eQ\langle T_q^{(2)}(\nabla \mathbf{E})\rangle\end{aligned}$$

with the nuclear electric quadrupole coupling (NQC) tensor elements

$$eQ\langle T_0^{(2)}(\nabla \mathbf{E})\rangle = \chi_{aa}/2 \quad (4)$$

$$eQ\langle T_{\pm 2}^{(2)}(\nabla \mathbf{E})\rangle = (\chi_{bb} - \chi_{cc} \pm 2i\chi_{bc})/\sqrt{24} \quad (5)$$

The χ_{ij} are the NQC constants (NQCC); χ_{ab} and χ_{ac} have been neglected since the inertial axis a is very close to the NQC principal axis z as discussed later. The χ_{bc} term permits two NQC axes to be rotated against the b and c principal axes of the inertial tensor. A nonvanishing χ_{bc} will connect states with $\Delta K = 2$ and thus cause an hfs contribution to the K-doubling. However, its effect is usually concealed by a much larger inertial asymmetry contribution, so off-diagonal χ_{ij} can only be determined by comparing sets of χ_{ij} of the same nucleus in different isotopomers [20]. The smaller the inertial asymmetry, however, the more the χ_{bc} effect will be noticeable. On the other hand, in slightly asymmetric molecules the prinicipal axes of inertia often coincide with the principal inertial axes, and hence χ_{bc} is zero.

In [19] also the matrix elements for the spin-rotation interaction are given. Since H_2S_2 is not a radical, this interaction is not present; however, these matrix elements are of use here to describe the nuclear spin - rotation interaction after replacing N, S, and J by J, I, and F, respectively. The result is:

$$\begin{aligned}&\langle J'K'IF|H_{\text{NSR}}|JKIF\rangle = \\ &\frac{1}{2}\sum_{k=0}^{2}\sqrt{2k+1}(-1)^{I+J'+F+1+k} \\ &\times \sqrt{I(I+1)(2I+1)(2J+1)(2J'+1)}\begin{Bmatrix} F & J' & I \\ 1 & I & J \end{Bmatrix} \\ &\times \left[\begin{Bmatrix} k & 1 & 1 \\ J & J' & J \end{Bmatrix}\sqrt{J(J+1)(2J+1)} \right. \quad (6) \\ &\qquad \left. + \begin{Bmatrix} k & 1 & 1 \\ J & J' & J' \end{Bmatrix}\sqrt{J'(J'+1)(2J'+1)}\right] \\ &\times \sum_{q=-k}^{k}(-1)^{J'-K'}\begin{Bmatrix} J' & 1 & J \\ -K' & q & K \end{Bmatrix} T_q^{(k)}(C)\end{aligned}$$

with the nculear spin - rotation constants C_{ij}:

$$T_0^0(C) = -(C_{bb} + C_{cc} + C_{aa})/\sqrt{3} \quad (7)$$

$$T_0^2(C) = (2C_{aa} - C_{bb} - C_{cc})/\sqrt{6} \quad (8)$$

$$T_{\pm 2}^2(C) = \frac{1}{2}[(C_{bb} - C_{cc}) \pm i(C_{bc} + C_{cb})] \quad (9)$$

The magnitude of the hfs splittings were estimated assuming the dominant nuclear quadrupole hfs to have the same order as in $H_2{}^{33}S$ [18].

3. Experiment

The HSSH sample has been produced in the Institute for Anorganische Chemie of the University of Köln. The spectra of $HS^{33}SH$ have been recorded in natural abundance, i.e. about 1.4 percent of the H_2S_2. For observation of the lines between 70 and 200 GHz, the mm-wave spectrometer was used in the configuration previously described in [11]; the transitions beyond 200 GHz were measured using two phase-locked backward wave oscillators (Carcinotron, Thomson-CSF) as frequency source, one for the 200-250 GHz and one for the 260-300 GHz region. The measurements have been made at room temperature with a sample pressure of 25 - 40 μbar.

Table 1. HS^{33}SH : Portion of observed transition frequencies /MHz, together with estimates of their experimental uncertainties, observed-minus-calculated values and relative hyperfine intensities. A complete list is available from authors on request.

J'	K'_a	K'_c	F'	—	J''	K''_a	K''_c	F''	ν_{obs}	$\Delta\nu_{obs}$	o-c	rel.Int.
4	1	3	5.5		5	0	5	6.5	71210.296	0.030	0.042	0.318
4	1	3	2.5		5	0	5	3.5	71210.970	0.030	0.021	0.167
4	1	3	3.5		5	0	5	4.5	71212.010	0.030	0.006	0.207
4	1	3	4.5		5	0	5	5.5	71212.613	0.030	–0.012	0.258
3	1	2	4.5		4	0	4	5.5	84944.949	0.030	0.014	0.333
3	1	2	1.5		4	0	4	2.5	84946.278	0.030	0.024	0.143
3	1	2	2.5		4	0	4	3.5	84947.240	0.030	–0.000	0.191
3	1	2	3.5		4	0	4	4.5	84948.669	0.030	0.032	0.255
45	1	45	44.5		45	0	45	44.5	138297.079[a]	0.020	0.003[b]	0.247
45	1	45	45.5		45	0	45	45.5	138297.079[a]	0.020	0.003[b]	0.252
45	1	45	43.5		45	0	45	43.5	138297.579[a]	0.020	–0.005[b]	0.242
45	1	45	46.5		45	0	45	46.5	138297.579[a]	0.020	–0.005[b]	0.258
44	1	44	43.5		44	0	44	43.5	138368.135[a]	0.020	0.011[b]	0.247
44	1	44	44.5		44	0	44	44.5	138368.135[a]	0.020	0.011[b]	0.252
44	1	44	42.5		44	0	44	42.5	138368.628[a]	0.020	–0.003[b]	0.241
44	1	44	45.5		44	0	44	45.5	138368.628[a]	0.020	–0.003[b]	0.258
1	1	0	2.5		0	0	0	1.5	153642.793	0.030	–0.027	0.500
1	1	0	0.5		0	0	0	1.5	153644.436	0.030	–0.013	0.167
1	1	0	1.5		0	0	0	1.5	153651.417	0.030	–0.007	0.333
42	1	41	40.5		41	2	39	39.5	157630.915[a]	0.030	0.024[b]	0.241
42	1	41	43.5		41	2	39	42.5	157630.915[a]	0.030	0.024[b]	0.259
42	1	41	41.5		41	2	39	40.5	157631.368[a]	0.030	0.005[b]	0.247
42	1	41	42.5		41	2	39	41.5	157631.368[a]	0.030	0.005[b]	0.253
7	1	6	5.5		6	0	6	4.5	236112.983	0.020	–0.018	0.192
7	1	6	8.5		6	0	6	7.5	236113.353	0.020	–0.001	0.300
7	1	6	6.5		6	0	6	5.5	236113.853	0.020	0.007	0.223
7	1	6	7.5		6	0	6	6.5	236114.473	0.020	–0.007	0.259
51	1	51	50.5		50	2	49	49.5	276930.357[a]	0.020	–0.018[b]	0.247
51	1	51	51.5		50	2	49	50.5	276930.357[a]	0.020	–0.018[b]	0.252
51	1	51	49.5		50	2	49	48.5	276930.924[a]	0.020	–0.009[b]	0.243
51	1	51	52.5		50	2	49	51.5	276930.924[a]	0.020	–0.009[b]	0.257
50	4	47			51	3	49		279489.183[c]	0.020	–0.001	
50	4	46			51	3	48		279490.264[c]	0.020	–0.001	
9	2	7	7.5		10	1	9	8.5	282189.894[a]	0.020	–0.020[b]	0.211
9	2	7	10.5		10	1	9	11.5	282189.894[a]	0.020	–0.020[b]	0.286
9	2	7	8.5		10	1	9	9.5	282190.380[a]	0.020	0.028[b]	0.233
9	2	7	9.5		10	1	9	10.5	282190.380[a]	0.020	0.028[b]	0.258
52	1	52	51.5		51	2	50	50.5	290440.244[a]	0.020	0.014[b]	0.247
52	1	52	52.5		51	2	50	51.5	290440.244[a]	0.020	0.014[b]	0.252
52	1	52	50.5		51	2	50	49.5	290440.794[a]	0.020	0.008[b]	0.243
52	1	52	53.5		51	2	50	52.5	290440.794[a]	0.020	0.008[b]	0.257

[a] overlap of two hfs components; [b] calc. frequency is intensity weighted average – see text; [c] hfs not resolved.

Since it was clear from previous measurements on HSSH and HS^{34}SH that the more abundant isotopomers' spectra would overlap the low-J $^{r}Q_0$ branch of HS^{33}SH , the measurements were started with the $^{r}P_0$ branch. After the clear detection of two quartets at 71.2 and 84.9 GHz, further transitions belonging to the $^{r}P_1$, $^{r}R_0$, $^{r}P_2$ and $^{r}P_3$ branches could be rapidly found. The accuracy of the rotational and centrifugal distortion constants allowed us then to predict and identify the higher-J $^{r}Q_0$ branch transitions up to J = 45. Altogether, a total of 133 line positions were recorded, containing 264 partially overlapping transitions. Table 1 shows observed frequencies together with estimates of their experimental uncertainties and calculated relative intensities.

4. Data Analysis

The observed frequencies have been fitted in a least squares procedure to the Hamiltonian discussed above. Whereas the hyperfine splittings of higher J transitions could be fitted easily, the lower J transitions could not be reproduced at all by fitting the hfs constants χ_{aa}, χ_{bb}, and χ_{cc}. Introduction of the

Table 2. $HS^{33}SH$: Rotational constants/MHz.

Parameter	value
A	146 773.9320 (70)[a]
B	6 871.81625 (59)
C	6 869.11235 (65)
$D_J \times 10^3$	5.25250 (83)
$D_{JK} \times 10^3$	83.410 (34)
D_K	2.4283 (23)
$d_1 \times 10^6$	8.615 (36)
$d_2 \times 10^6$	–25.842 (20)
$H_J \times 10^9$	–1.57 (32)
$H_{JK} \times 10^9$	–28 (34)
$H_{KJ} \times 10^6$	2.5 (34)
$H_K \times 10^6$	207 (323)
$h_2 \times 10^{12}$	31.0 (134)
$h_3 \times 10^{12}$	3.53 (146)

[a] values in brackets: 3σ.

Table 3. $HS^{33}SH$: Hyperfine constants/MHz due to the ^{33}S nucleus determined in the present work, in comparison to ab-initio values by Palmer [17].

Parameter	Experimental[a]	SCF[b]	CI[b]
$\chi_{aa} = \chi_{zz}$	–36.28 (28)	–40.28	–38.83
$\chi_{bb} - \chi_{cc}$	–4.156 (79)		
χ_{bc}	28.88[c] (21)		
χ_{bb}[d]	16.063 (151)		
χ_{cc}[d]	20.219 (139)		
χ_{xx}[e]	–10.82[c] (25)	–4.87	–4.92
χ_{yy}[e]	47.10[c] (25)	44.62	43.56
$\theta_{bx} = \theta_{cy}$[e]	42.94°		
$C_{aa} + C_{bb} + C_{cc}$	0.059 (55)		
$2C_{aa} - Cbb - C_{cc}$	0.082 (83)		
$C_{bb} - C_{cc}$	–0.0069 (86)		
C_{aa}[d]	0.047 (44)		
C_{bb}[d]	0.0025 (104)		
C_{cc}[d]	0.0094 (130)		

[a] values in brackets: 3σ; [b] From [17]; [c] $\chi_{xx} < \chi_{yy}$ assumed following [17]; [d] derived value; [e] obtained from diagonalization of NQC tensor.

parameter χ_{bc} solved the problem immediately, as the o-c values in Table 1 show – we will discuss this finding below in somewhat more detail. Following [21], non-resolved lines have been fitted to the average of the calculated frequencies, weighted by their calculated intensities. This procedure allowed us to take advantage of the full spectrometer precision in the analysis, resulting in a σ of 14 kHz; the observed-minus-calculated (o-c) values are also given in Table 1. Table 2 shows the rotational and centrifugal distortion constants, and the hyperfine constants are given in Table 3, including three parameters due to nuclear spin-rotation interaction. Matrix elements not diagonal in J did not improve the fit and were subsequently neglected in the analysis.

5. Discussion

The rotational constants are well behaved in the sense that they average fairly well the corresponding HSSH and $HS^{34}SH$ values. The new and more interesting feature presented here is the hyperfine structure due to the ^{33}S nucleus. And here again, disulfane gives rise to an extraordinary behaviour. Since the molecule comes very close to an accidental prolate top, the asymmetry splitting is very small, especially for the lowest rotational levels. However, the molecular geometry (Fig. 1) is not close at all to a prolate symmetric top. This fact was noticed very early by the selection rules: $HS^{33}SH$ exhibits c-type spectra only, whereas a prolate symmetric top can only have a-type transitions.

To understand our findings concerning the ^{33}S hyperfine structure, one should recall the connection between nuclear quadrupole hyperfine interaction and the chemical bond. From Fig. 1 we see that the SSH bond angle does not differ much from 90°. Therefore,

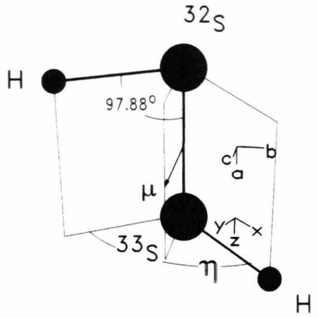

Fig. 1. Geometry of $HS^{33}SH$. The equilibrium SSH angle is taken from [9]. The orientation of the principal inertial axes a, b, c and the principal NQC axes x, y, z show a substantial rotation around the a axis. The dipole moment vector μ is parallel to the c axis. The z and a axes are almost parallel to the SS-bond, while the ^{33}S H bond comes close to the x axis. Therefore, twice the angle between the x and c axis should give a good estimate for the dihedral angle. We find $\eta \approx 94°$, in good agreement with η = 90.91° obtained in [11] for the ground state of $HS^{33}SH$.

one may assume two principal axes of the NQHFS to be close to the SS and the SH bond axes. While the SS axis nearly coincides with the a inertial axis, the SH bond is rotated about 45° versus the b and c axes. Thus one may expect χ_{bc} to be of considerable magnitude, and χ_{ab} and χ_{ac} to almost vanish. As discussed in the Hamiltonian section, the matrix element associated with χ_{bc} contributes to the asymmetry doubling. However, for most cases, its effect on the energies is not directly observable.

Now the case of $HS^{33}SH$ special in that a considerably large χ_{bc} value appears combined with an extremely small inertial asymmetry. This fact expresses again that the geometry of the bonds cannot belong to a molecule similar to a prolate top, despite of the inertial proximity to the prolate case. The K doubling is most noticeable in the $K_a = 1$ levels where the respective matrix elements contribute to the energies in first order, and the effect of the hyperfine structure will be most pronounced in the low J rotational levels. It is illustrative to regard the 1_{10} and 1_{11} levels. Figure 2 shows their energy contributions due to inertial asymmetry, diagonal, and off-diagonal NQC constants. The first observation is that the hyperfine structure is larger than the asymmetry doubling for this lowest K-split level. But whereas the diagonal NQC constants mix the two rotational sublevels, the χ_{bc} term not only changes the order of the hyperfine sublevels, but it contributes to the K doubling in a way that separates the 1_{11} and 1_{10} subgroups again. The dominant contribution to the K doubling of the $J = 1$, $K_a = 1$ arises from the non-coincidence between the principal inertial axes and the principal axes of the NQC tensor.

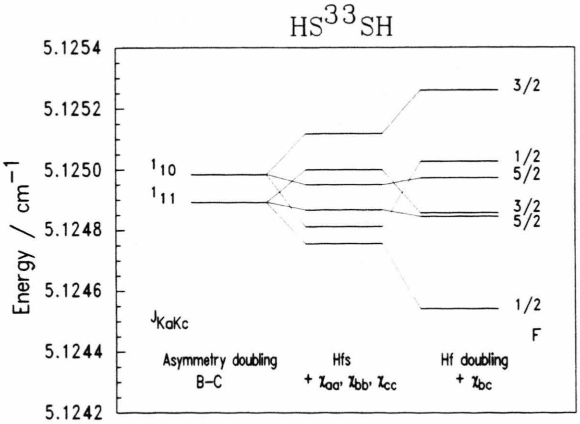

Fig. 2. Contributions to the 1_{10} and 1_{10} rotational levels in the ground state of $HS^{33}SH$. The hfs contributions diagonal in K are already larger than the asymmetry splitting and would mix the K doublets, if not the off-diagonal χ_{bc} separated them again. χ_{bc} is the dominant contributor to the K doubling in these levels.

The J-dependence of the hyperfine splitting with respect to the pure rotational energy levels with $K_a = 1$ can be seen in Figure 3. The effect of the off-diagonal χ_{bc} is visible for the low J rotational levels only. This explains why initially the higher J transitions could be well fitted without employing χ_{bc}. Figure 4 shows the relative frequency splittings in the transition frequencies of the $^{r}P_1$ branch. Incorporated spectra are examples of recorded transitions calling for the need of χ_{bc} to explain them.

It should be noted that the sign of χ_{bc} cannot be determined from the present measurements. In order to decide the proper choice of sign, additional information is required. In the course of writing this paper we became aware of an ab-initio paper by Palmer [17] who has calculated the ^{33}S NQCC for a series of molecules, inluding $HS^{33}SH$. His NQCC are given in the NQC principal axis system, with the z-axis almost coinciding with the a axis and the x axis close to the SH bond. He found that the latter axis has the smallest NQCC, while χ_{yy} is the largest. From our values of χ_{bb}, χ_{cc}, and χ_{bc}, the χ_{xx} and χ_{yy} can be obtained by diagonalization of the NQCC tensor:

$$\begin{pmatrix} \chi_{xx} & 0 \\ 0 & \chi_{yy} \end{pmatrix} = R_\theta^{-1} \begin{pmatrix} \chi_{bb} & \chi_{bc} \\ \chi_{bc} & \chi_{cc} \end{pmatrix} R_\theta, \qquad \text{where } R_\theta = \begin{pmatrix} \cos\theta & -\sin\theta \\ \sin\theta & \cos\theta \end{pmatrix}. \tag{10}$$

Besides χ_{xx} and χ_{yy}, this yields also the angle θ between the principal axes of inertia and the principal NQC axes. In Table 3, our experimental hyperfine constants can be compared with the ab-initio values from [17]; the NQCC show a good qualitative agreement between experimental and theoretical values. Following Palmer, we assign $\chi_{xx} < \chi_{yy}$; this choice results in a positive χ_{bc} and an angle θ of 42.94° between b and x axis[1]. From Fig. 1, one can easily

---

[1] The opposite assignment yields an angle of 47.06° between b and x axis and the estimate for η would become 86°.

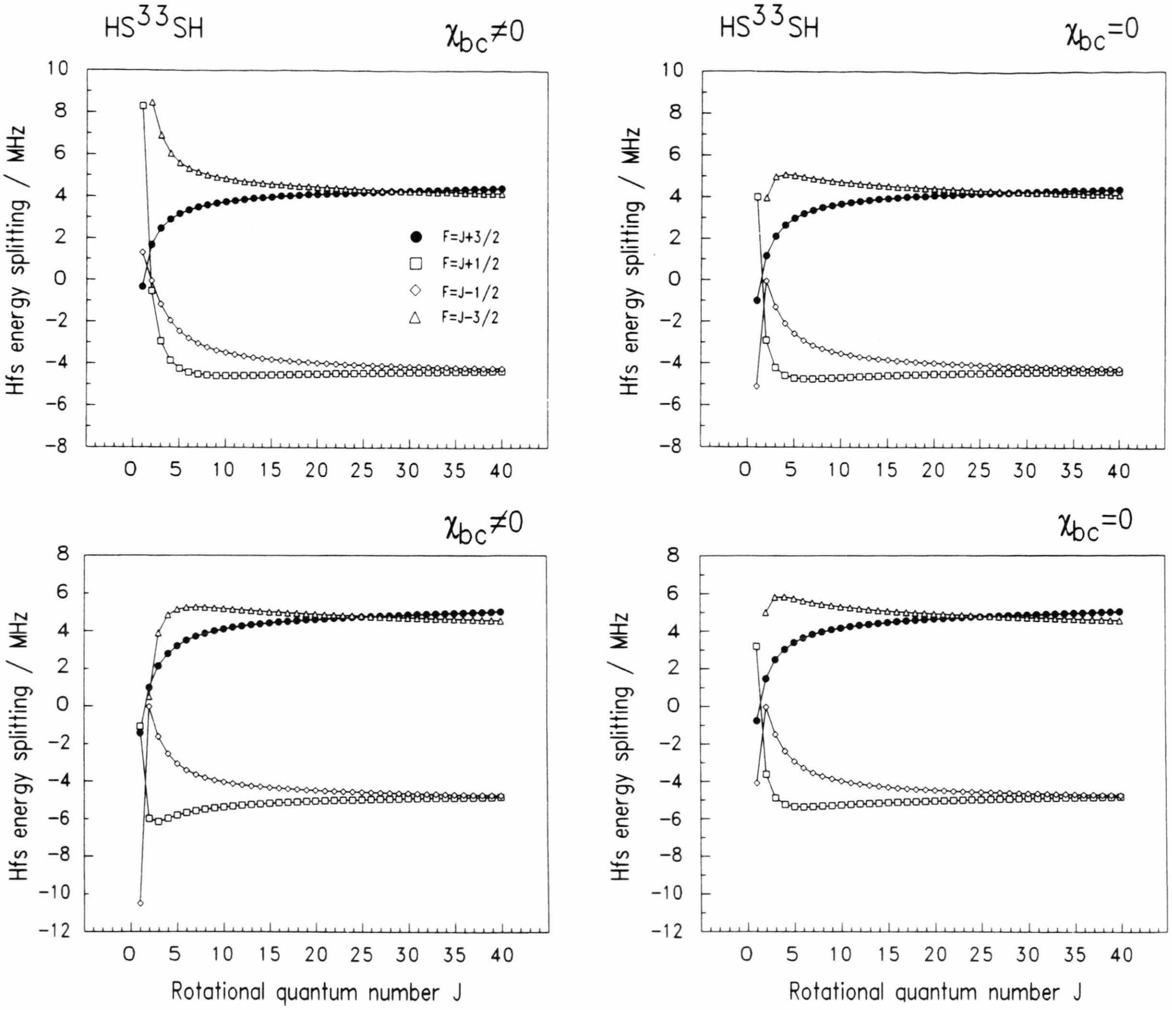

Fig. 3. J-dependence of calculated hyperfine energy splittings to the upper (above) and lower (below) components of $K_a = 1$ states. To the *left*, the hyperfine doubling contribution χ_{bc} is included, but neglected in the diagrams on the *right* side. Only low-J rotational levels are strongly affected by hyperfine doubling.

recognize the approximate relationship:

$$\eta \approx 2(90^\circ - \theta). \tag{11}$$

This relation would be exact if the SH axis coincided with the x axis, and the SS bond with the z axis. This condition is not exactly fulfilled, but our estimate of 94° for η is fairly close to the 90.91° obtained by Behrend [11] for the ground state of HSSH, based on the rotational constants of several other isotopomers. This fact underlines the overall consistency of the experimental data on disulfane now available from rotational spectroscopy.

6. Conclusion

Once again, disulfane has given rise to a special spectral feature. The first determination of the HS^{33}SH rotational spectra has shown that for low J rotational quantum numbers, the K-doubling is dominated by contributions from the ^{33}S quadrupole hyperfine interaction rather than from the asymmetry of the inertia tensor. The reason is found in the combination of an extremely small inertial asymmetry with a strong rotation of the NQC principal axes against the principal inertial axes. From the NQCC we derive a dihedral angle of 94°, in good agreement with

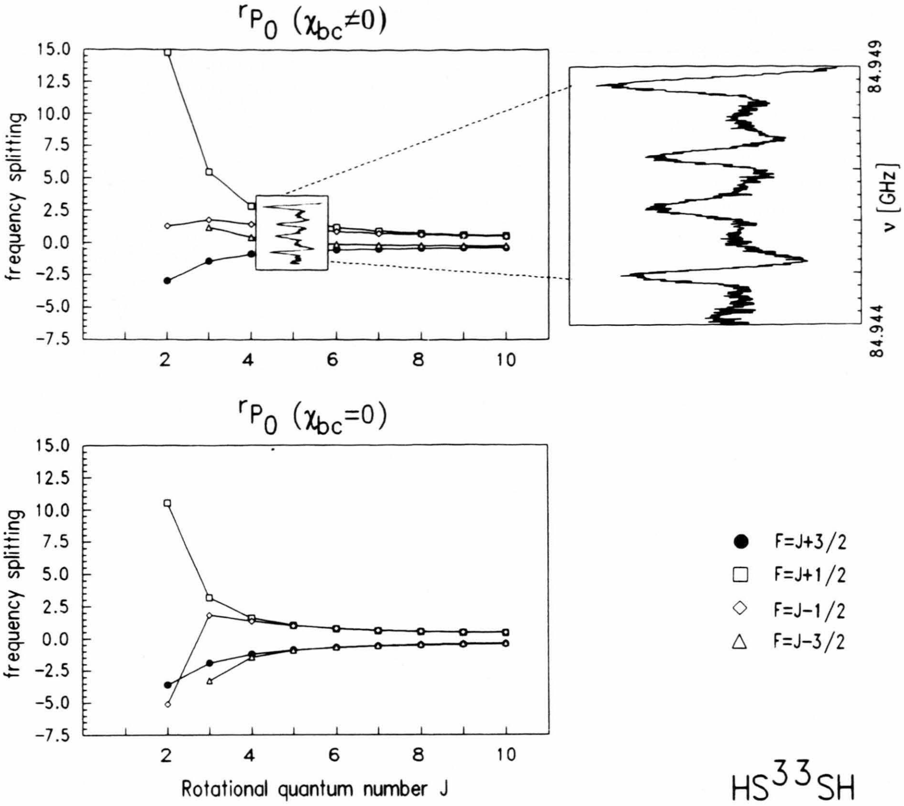

Fig. 4. J dependence of hyperfine splittings in MHz for the strongest hyperfine components of $^{r}P_0$ branch transitions. The incorporated observed spectrum ($J = 4$) shows an example where successfull fitting requires the introduction of χ_{bc}.

a previous value based on the rotational constants of other isotopomers. On the basis of the present experimental data, we had to recur to an ab-initio calculation for the probable assignment of χ_{xx} and χ_{yy}. As a final remark, we would like to mention that this assignment can be verified on experimental basis by determination of the NQCC in H^{33}SSD and HS^{33}SD , since for these isotopomers the NQCC and inertial principal axes should almost coincide. Therefore, mm-wave spectra of H^{33}SSD and HS^{33}SD will be of interest.

Acknowledgements

The authors thank Dr. J. Hahn and R. Klünsch of the Institute for Anorganische Chemie for the sample preparation. Valuable discussions with Dr. J. Behrend are thankfully acknowledged. And we appreciate helpful comments on the manuscript by Dr. K. M. T. Yamada. This work was supported in part by the Deutsche Forschungsgemeinschaft via grant SFB 301.

[1] G. Winnewisser, M. Winnewisser, and W. Gordy, Bull. Amer. Phys. Soc. **11,** 312 (1966).
[2] G. Winnewisser, M. Winnewisser, and W. Gordy, J. Chem. Phys. **49,** 3465 (1968).
[3] G. Winnewisser, J. Mol. Spectrosc. **41,** 534 (1970).
[4] G. Winnewisser, J. Chem. Phys. **56,** 2944 (1972).
[5] G. Winnewisser, J. Chem. Phys. **57,** 1803 (1972).
[6] G. M. Plummer, G. Winnewisser, M. Winnewisser, J. Hahn and K. Reinartz, J. Mol. Spectrosc. **126,** 255 (1987).
[7] Š. Urban, E. Herbst, P. Mittler, G. Winnewisser, K. M. T. Yamada, and M. Winnewisser, J. Mol. Spectrosc. **137,** 327 (1989).
[8] P. Mittler, K. M. T. Yamada, and G. Winnewisser, Chem. Phys. Lett. **170,** 125 (1990).
[9] J. Behrend, P. Mittler, G. Winnewisser, and K. M. T. Yamada, J. Mol. Spectrosc. **141,** 265 (1990).
[10] J. Behrend, P. Mittler, G. Winnewisser, and K. M. T. Yamada, J. Mol. Spectrosc. **150,** 99 (1991).
[11] J. Behrend, Dr Thesis, University Köln 1993.
[12] T.-K. Ha, J. Mol. Struct. **122,** 225 (1985).
[13] F. Grein, Chem. Phys. Lett. **116,** 323 (1985).
[14] D. Dixon, D. Zeroka, J. Wendoloski, and Z. Wasserman, J. Phys. Chem. **89,** 5334 (1985).
[15] M. Aida and C. Nagata, Theor. Chim. Acta **70,** 73 (1986).
[16] C. J. Marsden and B. J. Smith, J. Phys. Chem. **92,** 347 (1988).
[17] M. H. Palmer, Z. Naturforsch. **47a,** 203 (1992).
[18] A. H. Saleck, M. Tanimoto, S. P. Belov, Th. Klaus and G. Winnewisser, J. Mol. Spectrosc. **171,** 481 (1995).
[19] I. C. Bowater, J. M. Brown, and A. Carrington, Proc. Roy. Soc. London **A 333,** 265 (1973)
[20] W. Gordy and R. L. Cook, Microwave Molecular Spectra, 3rd ed, John Wiley, New York 1984.
[21] H. D. Rudolph, Z. Naturforsch. **23a,** 540 (1968).